Chapter 13

Anti-Corrosive Properties and Physical Resistance of Alkyd Resin–Based Coatings Containing Mg-Zn-Fe Spinels

Kateřina Nechvílová, Andrea Kalendová and Miroslav Kohl

Additional information is available at the end of the chapter

http://dx.doi.org/10.5772/65545

Abstract

The anti-corrosive and physical properties of organic coatings containing spinel pigments $Mg_{0.2}Zn_{0.8}Fe_2O_4$ wer studied. Pigments exhibiting different particle morphologies were synthesized by high-temperature solid phase reactions. Core-shell pigments containing Fe-Mg-Zn ferrite shells deposited on non-isometric particles of mineral cores consisting of layered silicates were also prepared. The pigments were used in paints, the pigment volume concentrations in the binder being 5, 10 and 15%. Anti-corrosive efficiency was investigated for paint films containing one of three ferro-spinel ($Mg_{0.2}Zn_{0.8}Fe_2O_4$)-based pigments or one of two core-shell pigments consisting of Fe-Mg-Zn shell and lamellar silicate-based cores. The paint properties were examined by accelerated corrosion tests and by physico-mechanical tests. The relationships between the pigment particle shape and the paint properties were examined. The effect of the pigment particle morphology on the mechanical properties of the paint films was also investigated. The dependence of the paint film properties on the pigment volume concentration was studied and the optimum concentrations providing the most efficient anti-corrosive protection were determined for each pigment.

Keywords: anti-corrosive pigment, organic coating, spinel, ferrite, core-shell pigment, accelerated corrosion test

1. Introduction

Metals are routinely protected against atmospheric corrosion by coating with pigmented paints possessing anti-corrosive properties [1]. Development of non-toxic anti-corrosive pigments for paints protecting the substrate efficiently against corrosion is a major trend in the science and technology of organic coating materials. The goal of research in this area is to develop non-toxic pigments possessing a high anti-corrosive efficiency with a view to replacing lead and chromium (VI)-based pigments that used to be applied in the past [2–4]. One direction in this area focuses on chemical or physical modification of known pigments, typically of the phosphate type [3, 5]. New inorganic pigments or organic corrosion inhibitor are also developed [6]. Among rather new anti-corrosive pigments are spinel-type pigments, finding application as thermally stable colour pigments and also as anti-corrosive pigments to protect the substrate against corrosion [7, 8]. Owing to their stable structure, spinel pigments exhibit a high resistance against high temperatures and chemical effects [9]. Mixed oxides in the spinel form, particularly ferrites containing Ca, Zn, Mg and their solid solutions, applied in paints already assume a firm position in anti-corrosion protection of metals [10, 11]. More efficient than the spinel-structure ferrite-type pigments with a combination of two cations in the lattice structure ($ZnFe_2O_4$, $MgFe_2O_4$) are second-generation spinel pigments with three cations ($Mg_{1-x}Zn_xFe_2O_4$ and $Ca_{1-x}Zn_xFe_2O_4$) [12]. Ferrite pigments are reactive particles on the surface in which there occur chemical reactions leading to the formation of less aggressive substances and a protective film during the diffusion of the corrosion substances through the polymeric film [13].

The protective properties of organic coatings are dependent, among other factors, on their impermeability to liquids and gases [14–16]. Protective film impermeability to liquids and gases can be improved by using non-isometric fillers [17, 18], e.g. micaceous iron oxide (specularite) [19–21]. **Figure 1** shows schematically the effect of non-isometric pigment particles on the physical properties of the paint films, consisting in an improvement of the mechanical properties of the films, reduction of the rate of diffusion through the films and protection of the binder against UV radiation [22, 23].

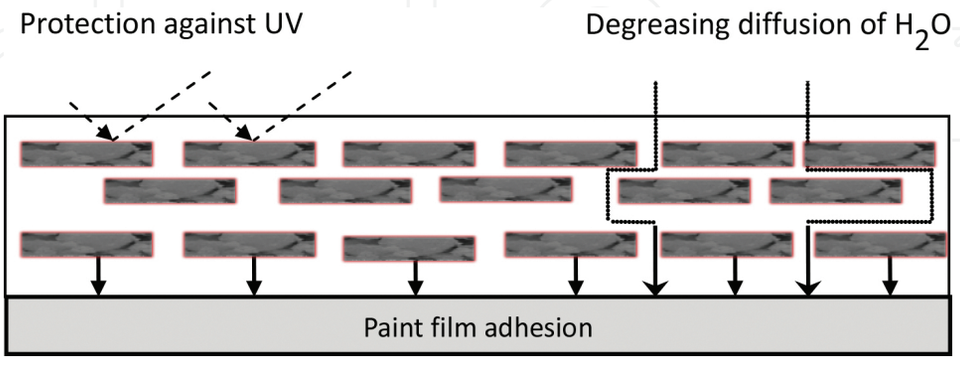

Figure 1. Pigment particles with a lamellar morphology in the paint film [29, 30].

Among pigments exhibiting non-isometric particle morphology are also some core-shell pigments [24]. The composition of both the core and the shell can be very diverse. Inorganic

http://dx.doi.org/10.5772/65545

substances or metal powders are frequently used [25, 26]. Among assets of core-shell pigments is their economy, because raw materials from natural sources can often be used as the cores [27]. Control of the particle morphology, owing to which the product particles retain the shape of the initial core particles, is another reason why such pigments are used [28].

An ideal anti-corrosive pigment will not only possess good corrosion-inhibition properties but it will also have a favourable effect on the paint film's mechanical resistance [31, 32]. Among candidates that are studied in this context are pigments based on mixed oxides, specifically ferrites. The development of pigments whose primary particles possess a non-isometric, lamellar shape represents another direction in the development of anti-corrosion pigments. Such pigments, with their alkaline properties, can enhance both the barrier and inhibiting mechanisms of the protective paint system [33]. Examples include Zn, Ca, Mg ferrites with a lamellar, non-isometric particle shape which, apart from their anti-corrosion properties, improve the paint film's mechanical properties such as bending strength, elasticity and adhesion to the substrate [34]. The resulting ferrite spinels were found to retain particle morphology of the initial iron oxides [35]. The most efficient anti-corrosive ferrites include ferro-spinels containing zinc and magnesium in specific ratios [9, 36]. It has been found that ferrites with Mg^{2+} and Zn^{2+} as the divalent cations exhibit a very good anti-corrosive efficiency, especially if their molar ratio is 0.2:0.8 [37]. The studies are continued in this work, where one of the phenomena investigated was the effect of the particle size on the properties of the protective paint films based on a modified alkyd resin.

The aim of this study was to synthesize and investigate the properties of Mg-Zn-Fe ferro-spinel-based pigment possessing different particle morphologies with the goal to prepare such paints pigmented with them as they exhibit very good physical and anticorrosive properties. Core-shell pigments containing silicate cores and Mg-Zn-Fe shell were also prepared and studied with focus on their properties in protective coatings in a simulated corrosive environment. The particle morphology of such pigments is dictated by the core particle's shape and size, affecting the physical properties and barrier properties of the organic coating in corrosive environments. In order to get a deeper insight into the role of the pigment in the paint, the effect of the core material structure and chemical composition as well as the effect of the pigment concentration on the barrier capacity and the physical and anti-corrosive properties of the paint in the corrosive environment should be investigated [38, 39]. Layered silicates, specifically talc and calcined kaolin, exhibited differences in the composition, physical properties of their surface and particle texture, which may affect the pigment properties in the paints. Talc, $Mg_3(OH)_2$ (Si_4O_{10}), is a soft hydrophobic mineral (hardness 1 on the Mosh scale) with lamellar particles. Calcined kaolin obtained by calcination of the mineral kaolinite $Al_4(OH)_8$ (Si_4O_{10}) at 600°C contains morphologically diverse particles, largely lamellar, is harder than talc and contains more structural phases (largely mullite and quartz) [40–42]. All that may play a role in the overall anti-corrosive properties of the core-shell pigments [43, 44]. Core-shell pigments represent an economical solution for the synthesis of anti-corrosive pigments [27] obtained by the high-temperature reaction. Moreover, talc and kaolin are natural materials which are reasonably well available and are environmentally and toxicologically acceptable.

2. Experimental methods and procedures

2.1. Pigment synthesis

The pigments were formulated as the oxides $Mg_{0.2}Zn_{0.8}Fe_2O_4$ possessing a spinel structure. Efforts were made during the synthesis of the ferrite $Mg_{0.2}Zn_{0.8}Fe_2O_4$ ("pigment ***A***") to achieve (create) the spinel structure and isometric particles. Therefore, α-Fe_2O_3 (hematite), whose particles are regularly nodular, was used as the starting material. The aim of the synthesis of the next $Mg_{0.2}Zn_{0.8}Fe_2O_4$ ferrite ("pigment ***B***") was to obtain a with a non-isometric—specifically needle-shaped—particle morphology. Goethite α-FeO (OH), with needle-shaped particles, was used as the ferric oxide source. The third $Mg_{0.2}Zn_{0.8}Fe_2O_4$ ferrite ("pigment ***C***") was prepared by an identical procedure with the aim to prepare a non-isometric spinel pigment with a lamellar particle shape. Specularite, a ferric oxide Fe_2O_3 with a lamellar particle structure, was used as the starting material. The aim of the synthesis of the core-shell pigments with Mg-Zn-Fe shell was to coat the mineral core with a functional layer of mixed Mg-Zn-Fe oxides in the 0.2:0.8:2.0 ratios. Calcined Kaolin and talc $Mg_3(OH)_2(Si_4O_{10})$, i.e. materials exhibiting a lamellar particle shape, were used as the mineral carriers (cores). The core-shell pigments were synthesized by applying the matrix core (kaolin, talc)-to-mixed oxide (Mg-Zn-Fe) shell weight ratio 1:1.

The incoming materials were homogenized for 45 minutes, not only to obtain intimate mixtures but also to achieve mechanical-chemical activation of the materials, enhance contact of the particles in the powder mixture and increase the contact area for the reaction [4]. The high-temperature reaction was achieved by reaction mixture calcination in an electric furnace. The process was conducted as a two-stage procedure: the pigments were first calcined at 1000°C for 2 hours and then at 1180°C. The calcination temperatures were selected based on previous X-ray analysis of the products of tentative experiments. The resulting calcined material was multiply rinsed with distilled water. In order to obtain the right pigment particle size for use in paints, the calcinate was subjected to wet milling in a planetary ball mill (Pulverisette 6, Nietzsche, Germany). Accommodated in a milling vessel made of a zirconium silicate ceramics, the material was milled at 480 rpm for 420 minutes. The milling bodies were rollers made of the same ceramic material. The finely ground pigments were rinsed with water again and dried at 105°C in a laboratory-scale electric furnace. The core-shell pigments (or the mixed oxides forming the functional layer on the core) were also synthesized by high temperature solid-phase reaction, viz. by two-stage calcination like the non-core ferrites [43, 44].

Structural purity of the products was checked and their X-ray diffraction spectra were measured on a D8 Advance Diffractometer (Bruker AXS). The pigment particle surface and shape were examined on a JEOL-JSM 5600 LV scanning electron microscope (JEOL, Japan) [6].

2.2. Measuring the anticorrosion efficiency of the pigments in paints

In order to assess their potential anti-corrosion efficiency, the pigments were added to a solution of an alkyd resin modified with soy oil (density 1.1 g/cm^3, dry matter fraction 58.9%). The pigment volume concentrations (PVC) selected for the paints were 5, 10 and 15%. The

http://dx.doi.org/10.5772/65545

PVC/CPVC ratio (CPVC = critical PVC) was invariably adjusted to 0.35 by using limestone ($CaCO_3$) as an anti-corrosive-neutral filler. Cobalt octoate at a fraction of 0.3 wt.% was used as the siccative. The paints were prepared by dispersing the powdered pigments in the liquid binder in a Dispermat CV pearl mill. Test samples were prepared by coating test steel panels (deep-drawn cold-rolled steel manufactured by Q-panel, UK) 150 mm × 100 mm × 0.9 mm size with the paints by means of a box-type application ruler 200 μm slot width as per ISO 1514. The dry film thickness (DFT) was measured as per ISO 2808. Ten panels were prepared for each paint. A thin line 7 cm long and penetrating as deep as the substrate was cut into the paint film by using a sharp blade. Paint films were also prepared on polyethylene sheets, allowed to dry and peeled off and cut to pieces, 1 mm × 1 mm size. Such unsupported films were used to prepare 10% aqueous suspensions of the paint films in redistilled water [45].

The cyclic corrosion test in an environment with condensing water and SO_2 was performed as per CSN EN ISO 3231. This test consisted of 24-hour cycles comprising condensation of distilled water with SO_2 (0.2 mg/l) at 36°C for 8 hours followed by drying at 23 ± 2°C for 16 hours. The samples were evaluated after 1392 test hours. The corrosion tests were evaluated in accordance with the standards ASTM D 714-87, CSN ISO 2409, ASTM D 610-85 and ASTM D 1654-92. The following corrosion effects were assessed: formation (= size and frequency of occurrence) of blisters on the film surface and near the test cut made in the film; extent of substrate metal surface corrosion (corrosion-affected surface area fraction in %); and propagation (in mm) of corrosion in the vicinity of the test cut. Anti-corrosion efficiency on the 100–0 scale (100 = excellent anti-corrosion efficiency, 0 = poor anti-corrosion efficiency) was assigned to the corrosion effects in an environment with SO_2 [46].

2.2.1. Determination of corrosion-induced steel mass loss in aqueous extracts of the pigments

In this test, steel panels of defined size and known weight were submerged for 10 days in filtrates of 10 wt.% aqueous suspensions of the powdered pigments tested. The observed corrosion weight losses were converted to relative data (%) with respect to the values in water. The relative data obtained from the suspensions of the powdered pigments are denoted X_{corrp}. Relative corrosion losses (X_{corrf}) of steel panels exposed to 10% aqueous extracts of the loose pigmented paint films during 10 days were also measured [47, 48].

2.2.2. Effect of the pigments on the physico-mechanical properties of the organic coatings

The following tests were performed on the paint films: resistance to bending over a cylindrical mandrel; resistance to the cupping test (Erichsen test); resistance to a weight dropping on the reverse side of the test panels and adhesion (cross-cut test, or lattice test, knife spacing 1 mm). Degree of adhesion of the paints (ISO 2409) was performed by the cross-cut test. Impact resistance (ISO 6272) measured the maximum height of free drop of a weight (1000 g) at which the paint film still resisted damage. Resistance of the paint film against cupping (ISO 1520) was made in an Erichsen cupping tester. Resistance of the coating during bending over a cylindrical mandrel (ISO 1519) provides the largest diameter of the mandrel (in mm) causing disturbance of the paint film when the test panel is bent over it [49]. The results of the tests were used to calculate the overall physical-mechanical efficiency, i.e. overall paint film

resistance to mechanical effects. A resistance score on the 100–0 scale (100 = excellent resistance, 0 = poor resistance) was assigned to each test result. The overall physical-mechanical resistance of the paints (M_E) was calculated as the arithmetic mean of the cohesion score from the bending test on the cylindrical mandrel, the resilience score from the impact test, the degree of adhesion score and the strength score from the cupping [50].

The starting hematite was also examined (pigment ***F***). The non-pigmented organic coating material was subjected to the mechanical resistance tests and corrosion tests as well.

3. Results and discussion

3.1. Pigment morphology and structure

Morphology of the pigment particles synthesized is shown in the SEM photographs in **Figure 2**. The aim of the synthesis of the pigments ***A***, ***B*** and ***C*** was to obtain pigments possessing the spinel structure whose chemical formula is $Mg_{0.2}Zn_{0.8}Fe_2O_4$. Mixed spinel ferrites containing zinc and magnesium cations constituted the majority phases. The magnesium atoms can be iso-morphically substituted by zinc atoms, owing to which the mixed spinels can be formed across an unlimited range of concentrations. The magnesium-to-zinc cation ratio could not be determined precisely from the analysis because the lattice parameters in $MgFe_2O_4$ and $ZnFe_2O_4$ approach each other and the diffraction lines may overlap. The X-ray diffraction analysis of the pigments ***A***, ***B*** and ***C*** did not exhibit any crystal phases of the starting materials; in other words, the starting materials had completely reacted to the products. These results are consistent with [37]. Furthermore, the three spinel types were synthesized with a view to obtaining pigments $Mg_{0.2}Zn_{0.8}Fe_2O_4$ possessing different particle shapes, making use of the different particle shapes of the starting ferric oxide types: the particles of pigment ***A*** were isometric, the particles of pigment ***B*** were needle-shaped (acicular) and the particles of pigment ***C*** were lamellar. The three pigments are also referred to as isometric $Mg_{0.2}Zn_{0.8}Fe_2O$, acicular $Mg_{0.2}Zn_{0.8}Fe_2O_4$ and lamellar $Mg_{0.2}Zn_{0.8}Fe_2O_4$, respectively, throughout this text.

The core-shell pigment ***D*** ($Mg_{0.2}Zn_{0.8}Fe_2O_4$/*kaolin*) was prepared as a pigment whose non-isometric (lamellar) core particles of calcined kaolin are coated with a functional shell of the mixed oxide $Mg_{0.2}Zn_{0.8}Fe_2O_4$. For this, the starting materials for the shell were mixed in proportions providing the Mg-Zn-Fe cation ratio 0.2:0.8:2. Mixed oxides of aluminium, iron and magnesium were identified (the mixed oxide hercynite). The analysis gave evidence that chemical reactions had occurred between the kaolin surface and the remaining starting materials: indeed, the mixed oxide hercynite ($FeMg_3Al_2O_4$) contains the aluminium cation, which initially was present in the starting kaolin. In other words, a chemically bonded functional layer of mixed oxides had formed on the kaolin particles. The X-ray diffraction analysis showed that the pigment also included silicates ($MgSiO_3$) and crystalline silicon oxide (SiO_2) phases (cristobalite) from the starting kaolin. The resulting pigment ***D*** (simplified referred to as $Mg_{0.2}Zn_{0.8}Fe_2O_4$/*kaolin* or $Mg_{0.2}Zn_{0.8}Fe_2O_4/Al_6Si_2O_{13}$) exhibited a lamellar particle shape.

http://dx.doi.org/10.5772/65545

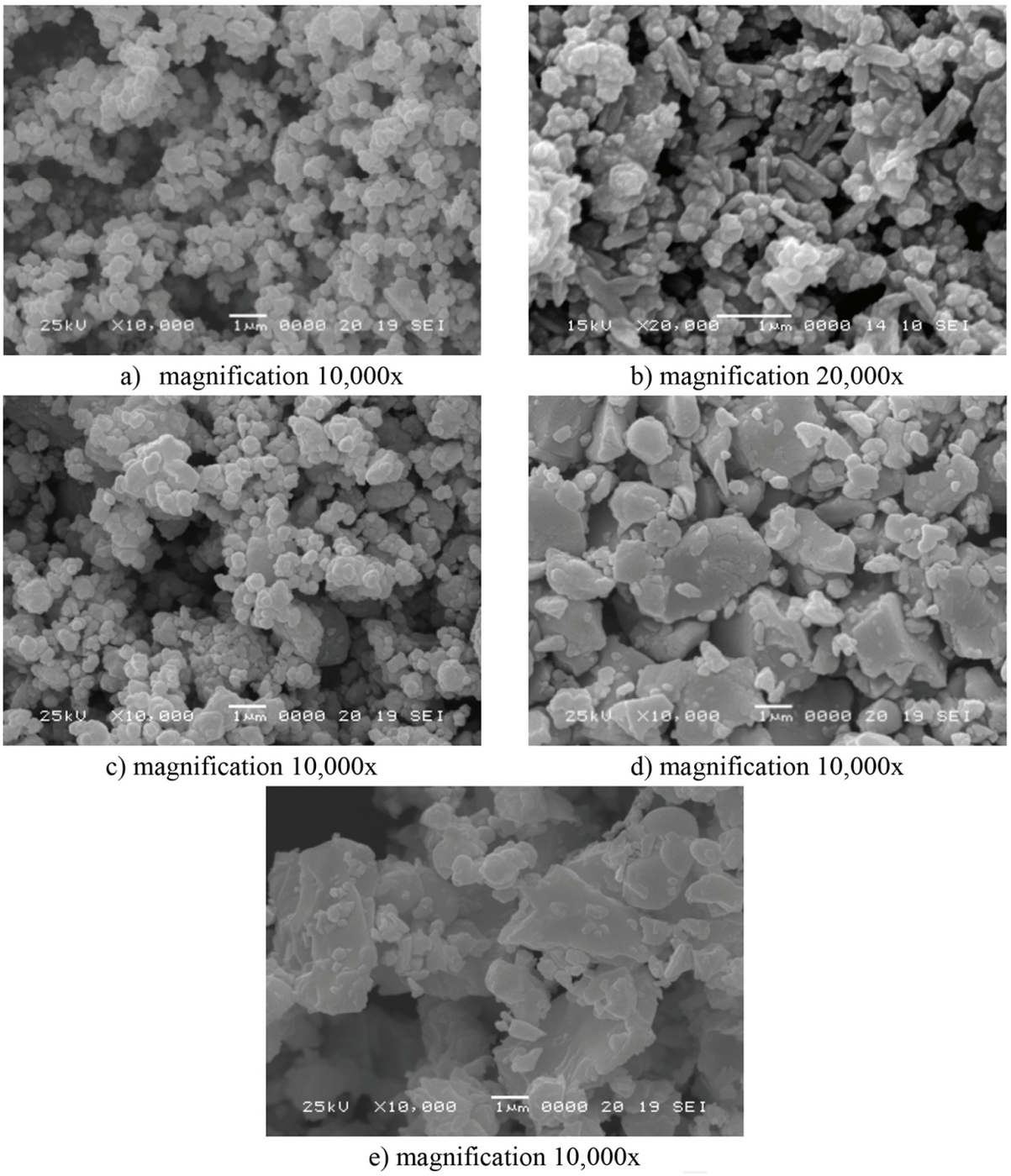

Figure 2. Morphology of the particles of tested pigments (SEM): (a) $Mg_{0.2}Zn_{0.8}Fe_2O_4$ isometric; (b) $Mg_{0.2}Zn_{0.8}Fe_2O_4$ acicular; (c) $Mg_{0.2}Zn_{0.8}Fe_2O_4$ lamellar; (d) mixed oxide Mg-Zn-Fe/kaoline; (e) mixed oxide Mg-Zn-Fe/talc.

Pigment ***E*** was synthesized with a view to obtaining a core-shell pigment where the mixed Mg-Zn-Fe oxide shell covers a mineral core possessing a lamellar particle structure, specifically talc $(Mg_3(OH)_2Si_4O_{10})$. The highest diffraction line belonged to the crystalline ferrite phase. As in the remaining pigments, isomorphic replacement of the zinc cation by a magnesium cation had occurred in this ferrite layer and so their precise ratio could not be

determined. Components of minor importance in this pigment included magnetite (Fe_3O_4) from the starting hematite and the silicon oxide cristobalite from talc in the core. The resulting pigment ***E*** (simply referred to as $Mg_{0.2}Zn_{0.8}Fe_2O_4/talc$ or $Mg_{0.2}Zn_{0.8}Fe_2O_4/Mg_3(Si_4O_{10})(OH)_2$) exhibited a lamellar particle shape.

3.2. Steel panel mass loss in aqueous extracts of the powdered pigments and of the loose pigmented films, and pH and conductivity of the pigmented aqueous extracts

Table 1 contains the calculated relative corrosion losses of the steel panels in aqueous extracts of the powdered pigments (X_{corrp}) and in aqueous extracts of the paint films (X_{corrf}), and pH values (pH_f) and specific electric conductivities (χ_f) of aqueous extracts of the loose paint films.

Pigment	**Corrosion losses***		**pH[a]** **pH_f (-)**	**Specific conductivity[b]** **χ (µS/cm)**
	X_{corrf} (%)	**$X_{corrp.}$ (%)**	**pH_{28}**	**χ_{28}**
A ($Mg_{0.2}Zn_{0.8}Fe_2O_4$) isometric	19.66	78.82	6.2 ± 0.01	190
B ($Mg_{0.2}Zn_{0.8}Fe_2O_4$) acicular	15.99	76.76	6.90 ± 0.01	195
C ($Mg_{0.2}Zn_{0.8}Fe_2O_4$) lamellar	4.29	33.31	7.90 ± 0.01	199
D (Mg-Zn-Fe) mixed oxide/kaolin	9.40	36.09	6.10 ± 0.01	200
E (Mg-Zn-Fe) mixed oxide/talc	9.98	43.93	6.70 ± 0.01	180
F (hematite) Fe_2O_3	28.15	89.87	5.10 ± 0.01	170
Water	-	100	-	-
Non-pigmented paint film	100	-	3.04 ± 0.01	216

*Parameters are given as arithmetic averages within three measured values.
[a]pH was measured with an accuracy of ±0.01.
[b]Conductivity was measured with an accuracy of ±0.5%.

Table 1. Relative steel mass losses due to corrosion in aqueous extracts of the powdered pigments (X_{corrp}) and in aqueous extracts of the loose paint films ($X_{corrf,}$) and pH and specific electric conductivity values (pH_f, χ_f) of the aqueous extracts of the loose paint films (PVC = 10%).

http://dx.doi.org/10.5772/65545

The corrosion loss data (X_{corp}) characterize the pigment's ability to affect the resistance of the metal to corrosion in the pigment extract, where ions passivating the metal surface are present to a larger or lesser extent. The data demonstrate that the corrosion phenomena are partly inhibited by the presence of the pigments [18]. Low steel losses by corrosion were observed with the core-shell pigments ***D*** (*mixed Mg-Zn-Fe oxide/kaolin*), and ***E*** (mixed *Mg-Zn-Fe oxide/talc*) and with the lamellar ferrite ***C*** (lamellar $Mg_{0.2}Zn_{0.8}Fe_2O_4$), viz. 36, 39 and 44%, respectively. Those (comparable) corrosion losses were related to the extracts' specific conductivities or pH levels [29]. Lower corrosion losses were observed with the core-shell pigments, where the silicate core and the silicate phases contributed favourably to corrosion protection of the steel panels [44].

The pigments also affected the pH and specific conductivity levels of the paint films pigmented with them. The alkaline nature of the pigments induced changes in the pH of the pigmented films compared to the non-pigmented film. The pigments shifted the pH values upwards due to the neutralization of the acid components of the binder [5, 51]. This effect was most pronounced for pigment ***C*** (lamellar $Mg_{0.2}Zn_{0.8}Fe_2O_4$), where pH_f was 7.9 (**Table 1**). The core-shell pigment ***E*** (mixed *Mg-Zn-Fe oxide/talc*) was a next pigment imparting an alkaline nature to the paint. The effects were reasonable, the pigments themselves inducing alkalinity in their aqueous extracts. Most acid (pH_f = 3.0) was the aqueous extract of the non-pigmented film. The conductivities of the aqueous extracts of the loose paint films were also affected by the pigments. The conductivity of the extract of the non-pigmented film was χ_f = 216 μS/cm. The conductivity was lower if a pigment was present. This was due to neutralization of the binder's acid components (R-COOH) giving rise to metallic soaps, where dissociation was suppressed [52]. This effect was marked, once again, with pigment ***C*** (lamellar $Mg_{0.2}Zn_{0.8}Fe_2O_4$) and, to a lesser extent, with the core-shell pigment ***E*** (*mixed Mg-Zn-Fe oxide/talc*) [43, 44].

The anti-corrosive efficiency of a paint film depends on the pigment's ability to release inhibiting components that are involved in the reactions inside the film and affect the diffusing environment. The corrosion losses in the suspensions of the organic films (X_{corrf}) containing anti-corrosive pigments provide information on the potential reactions occurring inside the paint in the liquid state, during the film formation and, to some extent, during the ageing of the cured film [48, 53]. The binder was an alkyd resin, a polyester modified by a fatty acid, which is well suited to the indirect examination of the behaviour of the ferrite and of the paint film. The carboxy groups in the binder were responsible for the acid nature of the aqueous extract of the film: the observed value was pH 3.1 when no pigment was present. However, if a pigment was present, the pH levels were largely as high as pH 6–8, due to the formation of metallic soaps inside the film [54]. Alkaline anti-corrosive pigments neutralized the acid groups in the binder [55]. This effect is basically similar to the inhibiting effect of minimum. Metallic soaps may also exhibit inhibiting properties at the protected metal–organic coating interface [6]. The alkyd binder contains both acid -COOH groups and an alkaline $Zn_{0.8}Mg_{0.2}Fe_2O_4$ pigment, as shown schematically in **Figure 3** [56]. Neutralization of the carboxy groups inside the film results in more or less neutral products: neutral metallic soaps M^{n+} ($^{-}$OOCR)n acidic metallic soaps M^{n+} (OOCR)n/RCOOH, and alkaline metallic soaps M^{n+} (O^{2-})x(OH^{-})y($^{-}$OOCR)z ($x/2 + y + z = n$). In the formulas, R is a hydrocarbon and M is a metal

(e.g. Zn, Mg) whose oxidation state [36]. The acid components of the binder that were released into the aqueous medium may also be neutralized by the alkaline extract of the anti-corrosive pigment [54, 57]. The low corrosion losses in the extracts of the loose paint films corroborated the results obtained with the extracts of the powdered pigments. The most marked active chemical protection was observed with the core-shell pigments ***D*** (*mixed Mg-Zn-Fe oxide/kaolin*) (X_{corrf} = 36.09%) and **C** (*lamellar* $Mg_{0.2}Zn_{0.8}Fe_2O_4$) (X_{corrf} = 39.31%).

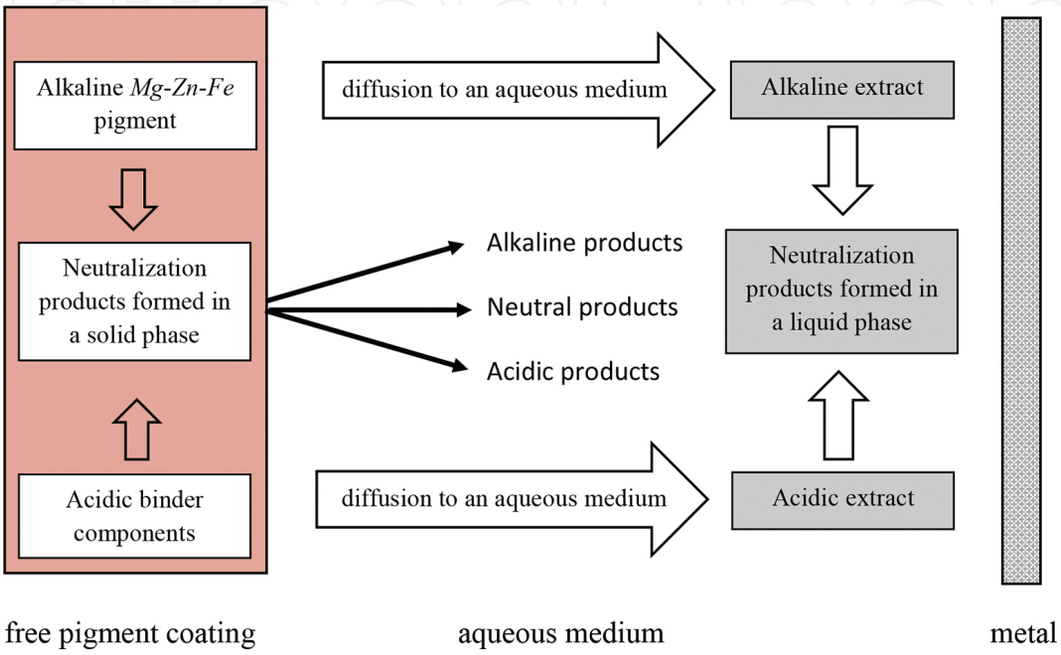

Figure 3. Schematic illustration of the processes running on extraction of alkyd coatings containing Mg-Zn-Fe pigment in an aqueous medium [54].

3.3. Mechanical resistance tests of the paint films containing the pigments

Outstanding mechanical properties constitute a precondition for good anti-corrosion efficiency of a paint film. **Table 2** presents the results of mechanical tests of the paints' films containing the pigments. The non-pigmented binder and a paint containing the starting ferric pigment ***F*** (hematite Fe_2O_3) were also measured as reference materials. Resistance in the dropping weight test was 100 cm for all the paint films. Similarly, resistance to the bending test was invariably less than 4 cm. Since the values were identical for all the pigments, they are not included in **Table 2**. The pigmented paints films exhibited very good resistance against mechanical stress at any PVC. The paint film was never disturbed when bent over the mandrel 4 mm in diameter. No defects were observed on the films after the test hammer was dropped from the largest height, i.e. 100 cm. Good results were also obtained for all of the pigments in the cross-cut test, any defects were negligible and nearly all of the films scored 1 in this test. The only pigment for which defects were observed on the lattice (particularly at higher PVC levels) was the core-shell pigment ***D*** (*mixed Mg-Zn-Fe oxide/kaolin*), and so the films scored 2. The films gave very good results also in the cupping test, no film disturbance was observed with a magnifying

glass after the body penetration to 8 mm distance. The paint film resistance in this test was PVC-dependent, viz. so that the resistance against penetration decreased slightly with increasing PVC. Pigment ***A*** (*isometric* $Mg_{0.2}Zn_{0.8}Fe_2O_4$) was an exception in this respect. **Table 3** also demonstrates that the highest resistance against the test body penetration was obtained with pigment ***B*** having needle-shaped particles (*acicular* $Mg_{0.2}Zn_{0.8}Fe_2O_4$), viz. 9.5 mm at PVC = 5%. Good results were also obtained with the core-shell pigment ***E*** (*mixed Mg-Zn-Fe oxide/talc*), where the film was disturbed at 9.4 mm.

Pigment	Cupping test* ISO 1520 (mm)	Cross-cut test* ISO 2409 (-)	Overall physico-mechanical resistance M_E
A	8.9	1	95
$Mg_{0.2}Zn_{0.8}Fe_2O_4$ isometric	8.8	1	95
	9.0	1	95
B	9.5	1	95
$Mg_{0.2}Zn_{0.8}Fe_2O_4$ acicular	9.2	1	95
	8.8	1	95
C	9.0	1	95
$Mg_{0.2}Zn_{0.8}Fe_2O_4$ lamellar	8.8	1	95
	8.5	1	95
D	9.3	1	95
Mg-Zn-Fe mixed oxide/kaolin	9.2	2	91
	8.8	2	91
E	9.5	1	95
Mg-Zn-Fe mixed oxide/talc	9.0	1	95
	8.8	1	95
F	8.7	1	95
hematite Fe_2O_3	8.9	1	95
	8.8	1	95
Non-pigmented paint film	8.8	1	95

*Parameters are given as arithmetic averages within three measured values.

Table 2. Results of mechanical tests of the paints containing the pigments synthesized and the reference pigment and of the reference paint (dry film thickness DFT = (60 ± 10) μm.

Nearly all of the paint films exhibited very good overall physico-mechanical resistance, their score was 95. Only the paints with the core-shell pigment ***D*** (*mixed Mg-Zn-Fe oxide/kaolin*) provided poorer cross-cut test at high PVCs and scored 91 only. The results give evidence that

owing to their morphological properties, the pigments tested do not detract from the mechanical resistance of the alkyd resin–based paints. These results are very important for practical applications of these pigments in paints.

Pigment	PVC (%)	Paint film		Steel panel		Calculated anti-corrosive efficiency
		Degree of blistering ASTM D 714-87		Corrosion in the cut (mm)	Metal surface corrosion (%)	
		Around the cut	On the film surface	ASTMD 1654-92	ASTMD 610-85	E_{SO_2}
A	5	2F	-	2.0–3.0	3	73
$Mg_{0.2}Zn_{0.8}Fe_2O_4$ isometric	10	4M	6F	2.0–3.0	33	49
	15	4MD	6F	1.0–2.0	50	42
B	5	4F	-	0.5–1.0	3	79
$Mg_{0.2}Zn_{0.8}Fe_2O_4$ acicular	10	4MD	-	0.5–1.0	1	71
	15	4MD	6F	0.5–1.0	16	54
C	5	6M	-	0.5–1.0	16	68
$Mg_{0.2}Zn_{0.8}Fe_2O_4$ lamellar	10	6F	-	0.5–1.0	16	68
	15	2F	2F	1.0–2.0	33	45
D	5	6D	8M	0.5–1.0	33	48
Mg-Zn-Fe mixed oxide/kaolin	10	6D	8M	0.5–1.0	>50	36
	15	4D	8MD	0.5–1.0	>50	30
E	5	8D	8M	1.0–2.0	>50	35
Mg-Zn-Fe mixed oxide/talc	10	8MD	8M	0.5–1.0	>50	43
	15	6MD	8M	1.0–2.0	>50	39
F	5	4M	8M	1.0–2.0	10	58
hematite Fe_2O_3	10	6MD	8D	1.0–2.0	>50	29
	15	6D	8D	0.5–1.0	>50	26
Non-pigmented paint film		4MD	2F	1.0–2.0	33	45

Table 3. Corrosion resistance of the paints with the pigments synthesized and with the reference pigment and of the reference paint, measured after 912 hours exposure of the steel panels coated with the paints in an atmosphere with SO_2, DFT = (85 ± 10) μm.

3.4. Corrosion tests of the pigmented paints

Table 3 lists the results of corrosion resistance measurements of the paint films in the atmosphere with condensed moisture and SO_2, obtained after 912 hours of exposure. Nearly all of the paint films had osmotic blisters on their surface after the exposure. The paint films with pigment ***C*** (*lamellar* $Mg_{0.2}Zn_{0.8}Fe_2O_4$) were most resistant in this respect, especially at PVC =10%, where no blisters were found on the film surface and a few small blisters only (6F) were observed around the test cut. The results observed when the pigment concentration was PVC

http://dx.doi.org/10.5772/65545

= 5% were also very good (6M). Equally good results were obtained with the paint containing pigment ***B*** (*acicular* $Mg_{0.2}Zn_{0.8}Fe_2O_4$). This was true particularly at PVC = 5%, whereas a higher occurrence of blisters was observed at higher concentrations. So, the blisters observed around the test cut at PVC = 10% were categorized as 4MD, as against the 4F score at PVC = 5%.

Similar behaviour was observed for the paint containing pigment ***A*** (*isometric* $Mg_{0.2}Zn_{0.8}$). Here, too, the resistance against blistering in the cut was poorer at higher concentrations: the scores at PVC = 5, 10 and 15% were 2F, 4M and 4MD, respectively.

The occurrence of blisters was more pronounced for the remaining paints. So, when the paint with the core-shell pigment ***E*** (*mixed Mg-Zn-Fe oxide/talc*) was used, the paint film surface was speckled with very small blisters (frequency of occurrence 8M). This applies to the entire PVC range. The effects were very similar with the core-shell pigment ***D*** (*mixed Mg-Zn-Fe oxide/kaolin*), where, in addition, more abundant (score 6D) blisters were found near the test cut. The poorest results were obtained by using the paint pigmented with the reference pigment ***F*** (hematite Fe_2O_3) at PVC =10% and at PVC = 15%, where the paint film surface was densely covered with very small blisters (score 8D). The differences in the extent of blistering on the various paint films are apparent from **Figure 4**.

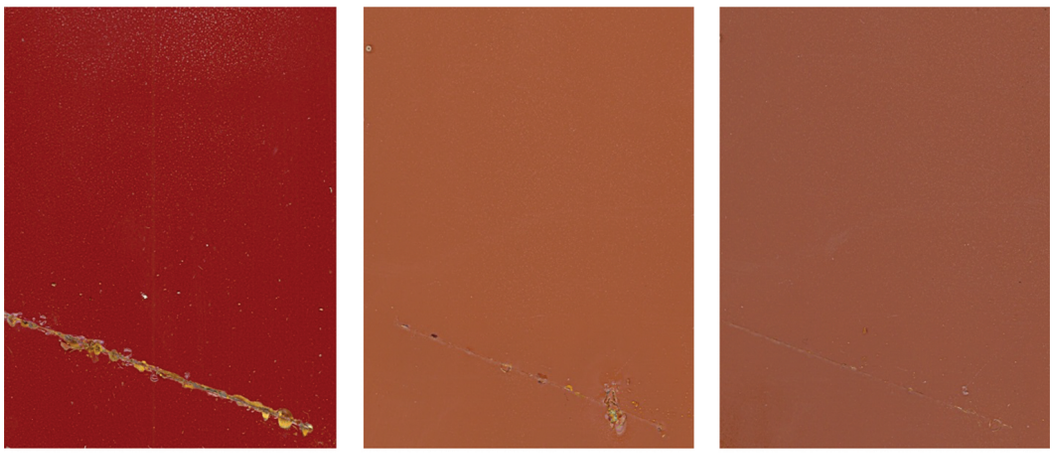

Figure 4. Photographs of the steel panels coated with paints containing: (a) pigment ***F*** (hematite Fe_2O_3) at PVC = 10%, (left); (b) pigment ***B*** (*acicular* $Mg_{0.2}Zn_{0.8}Fe_2O_4$) at PVC = 5% (middle); and (c) pigment ***C*** (lamellar $Mg_{0.2}Zn_{0.8}Fe_2O_4$) at PVC = 10% (right).

The paint films were removed from the steel panels in order to examine corrosion on the metal surface (beneath the initially present films) and corrosion propagation from the test cut. Corrosion in the test cut was similar for all of the paints. Appreciable corrosion propagation from the cut, reaching a 3 mm distance, was only observed for the paint with the isometric pigment ***A*** (*isometric* $Mg_{0.2}Zn_{0.8}Fe_2O_4$) at PVC = 5% and PVC = 10%, followed by the paint with the isometric reference pigment ***F*** (1.0–2.0 mm). The degree of corrosion was higher in this atmosphere than in the atmosphere with condensed moisture for nearly all of the paints. The best protection was provided by the paint with pigment ***B*** (*acicular* $Mg_{0.2}Zn_{0.8}Fe_2O_4$) at PVC = 10% and at PVC= 5%, the affected surface fraction being 1 and 3%, respectively. A comparable

protection was provided by the paint with pigment ***A*** (*isometric* $Mg_{0.2}Zn_{0.8}Fe_2O_4$) at PVC = 5% (corroded surface fraction 3%). This pigment exhibited a sharp drop of its protective capacity against corrosion beneath the film with increasing PVC: the affected fraction was as high as 50% at PVC=10%.

A comparison of the steel panel corrosion beneath selected paint films is presented in **Figure 5**. The photograph on the right shows the steel panel initially protected by the paint with pigment ***B*** (*acicular* $Mg_{0.2}Zn_{0.8}Fe_2O_4$) at PVC = 5%. The other two photographs show panels with appreciable degree of corrosion beneath the paint films.

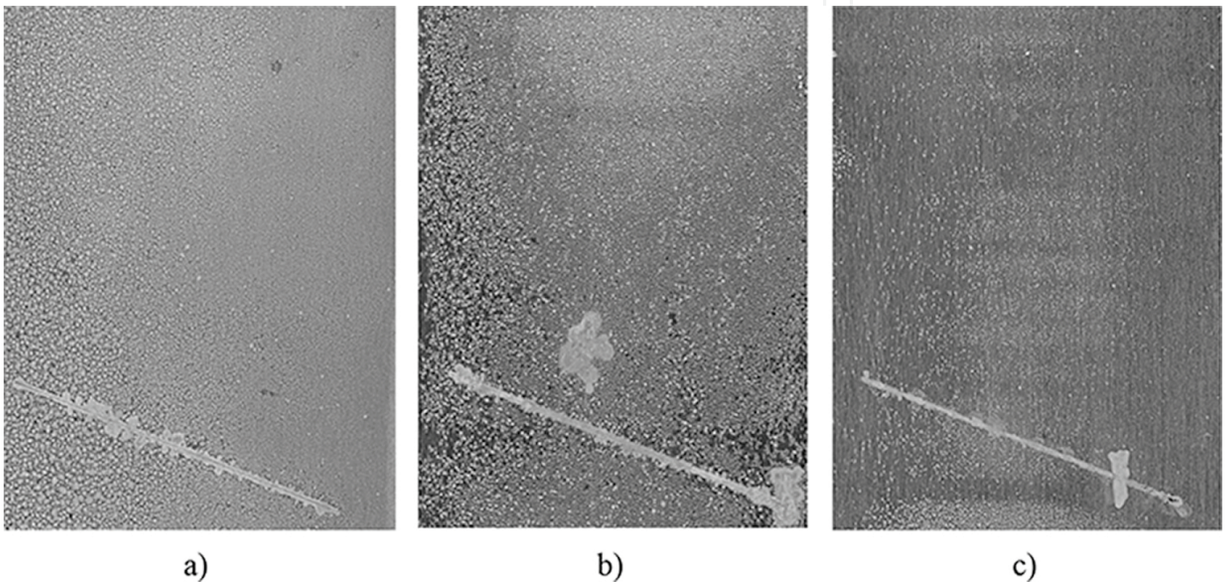

Figure 5. Photographs of the steel panels after removing the paint films: (a) pigment ***E*** (mixed *Mg-Zn-Fe oxide/talc*) at PVC = 15% (left); (b) pigment ***D*** (mixed *Mg-Zn-Fe oxide/kaolin*) at PVC = 15% (middle); (c) pigment ***B*** (acicular $Mg_{0.2}Zn_{0.8}Fe_2O_4$) at PVC = 5% (right).

The paint that was found most efficient in protection against corrosion in the environment with condensed moisture and SO_2 was that with the non-isometric pigment ***B*** (*acicular* $Mg_{0.2}Zn_{0.8}Fe_2O_4$). Paint films with this pigment were well resistant to blistering and efficiently protected the metal against corrosion. Favourably, this pigment is alkaline and can neutralize the strong acid aqueous medium acting on the paint film in the environment of the SO_2 chamber whose acidity is about pH 2. In the optimum arrangement, the needle-shaped pigment particles enhance cohesion of the paint and slow down diffusion of substances dissolved in the environment with condensing water [55]. The pigment is capable of forming soaps by reacting with the fatty acids (RCOOH) in the binder. Good resistance against blistering was also provided by the paint with pigment ***C*** (*lamellar* $Mg_{0.2}Zn_{0.8}Fe_2O_4$). At PVC = 15%, however, the protective capacity of this paint was as poor as that of the non-pigmented film—the affected metal surface fraction was 33%. In the optimum arrangement, particularly at low PVCs, the lamellar pigment particles enhance paint adhesion to the metal and it is more difficult for the corrosive medium to diffuse through the paint film. Similar results were obtained with the paint containing pigment ***A*** (*isometric* $Mg_{0.2}Zn_{0.8}Fe_2O_4$).

The following conclusion can be drawn from the observations in this corrosive environment:

- The non-isometric pigments exhibited the highest degree of protection against the formation of osmotic blisters on the paint film surface—higher than the isometric pigments.
- The isometric pigments (***A*** and ***F***) exhibit a higher ability to prevent corrosion of the metal at low PVCs. This may be associated with the nature of the corrosive environment: a paint film with a higher PVC is more porous and the SO_2 molecules penetrate faster and more readily through the film. As a result, the efficiency of the paints containing the isometric pigment particles at high concentrations decreases to the level of that of the non-pigmented film.
- Unlike the non-core-shell pigments, the core-shell pigments provide very low protection against metal surface corrosion.
- The chemically inactive pigment ***F***, acting by the barrier effect only, as well as the large particles of the core-shell pigments, is unable to completely prevent diffusion of the SO_2 molecules through the protective coating.
- Active protection against corrosion in the environment with SO_2 can be achieved by using a non-isometric pigment with small particles. The efficiency of such a pigment is higher than that of a core-shell pigment, which exhibits a larger particle size distribution.

The overall anti-corrosive efficiency was calculated for all the paint films tested. The most efficient in this respect was the paint with pigment ***B*** (*acicular* $Mg_{0.2}Zn_{0.8}Fe_2O_4$) at PVC = 5% (E_{SO_2} = 79) and at PVC = 10% (E_{SO_2} =71), followed by the paint with pigment ***C*** (*lamellar* $Mg_{0.2}Zn_{0.8}Fe_2O_4$) at PVC= 5% and 10% (E_{SO_2} = 68). Both pigment types exhibit a fairly uniform anti-corrosive efficiency. The corrosive environment contains mobile SO_2 ions [58] creating a strongly acid medium containing sulphite ions $\left(SO_3^{2-}\right)$ and sulphate ions $\left(SO_4^{2-}\right)$, and so a pigment with small particles exerting an alkaline effect is needed to attain a high corrosion resistance. Such a pigment will hinder diffusion through the paint film and neutralize the action of acid substances [52]. The paint with pigment ***A*** (*isometric* $Mg_{0.2}Zn_{0.8}Fe_2O_4$), was found efficient, its concentration, however, must be as low as PVC = 5% (E_{SO_2} =73).

The paint properties are not so favourable, in other words, the paint is not so efficient, if a core-shell pigment with lamellar particles is used. Such a paint is even less efficient than the coating material containing no pigment at all. Ideal for a paint exposed to the environment in question is a pigment with needle-shaped particles exerting an alkaline effect, which will also strengthen and reinforce the film.

4. Conclusions

Ferro-spinels (Zn-Mg-Fe) differing in the primary particle shapes were synthesized and added as pigments to a paint formula, and the paints containing them at various volume concentrations were investigated with respect to their anti-corrosive properties. Every property of a

pigmented paint is at its optimum at a specific pigment concentration; this applies particularly to the physical and anti-corrosive properties [37]. So it is possible to identify a pigment concentration at which a specific property is at its best or at which the overall anti-corrosive efficiency is at its maximum [59]. It is convenient that such pigment concentrations are usually not very high.

The spinels fall in the class of chemically acting pigments that help slow down corrosion processes on the metal surface beneath the paint film through their alkaline nature and by neutralization of the carboxy groups. The lamellar shape of the pigment particles enhances paint film adhesion to the substrate and its cohesion and reduces the formation of blisters on the paint film surface (and around the test cut). The pigmented paint films exhibited very good physico-mechanical properties, commensurable with those of the alkyd resin alone.

The best anti-corrosive efficiency in the accelerated corrosion test in the atmosphere with SO_2 was found for the paint containing the non-isometric pigment ***B*** (*acicular* $Mg_{0.2}Zn_{0.8}Fe_2O_4$) at PVC = 5%.

It follows from the results that the morphology the pigment particles plays a major role in the paints' anti-corrosive properties. Paints with non-isometric pigments gave better results than paints with isometric pigments during nearly all measurements. This is primarily due to the barrier effect to substances penetrating through the protective film. Furthermore, the aggressive substances in the penetrating medium come in closer contact with the pigment particles, which may result in neutralization of the former. The best combined anti-corrosive effect was found for pigment ***C*** with lamellar particles (lamellar $Mg_{0.2}Zn_{0.8}Fe_2O_4$). This pigment acted very favourably by the chemical inhibition mechanism; induced saponification in the alkyd resin owing to by its high alkalinity; and acted by the barrier effect. The core-shell pigments ***D*** (mixed *Mg-Zn-Fe oxide/kaolin*) and ***E*** (mixed *Mg-Zn-Fe oxide/talc*), which also exhibit very good anti-corrosive efficiency in many parameters, may also be used as convenient variants: they are less expensive than pigment ***C*** and contain less zinc because the mineral core represents a considerable fraction of the pigment particle weight.

Paints with the pigments tested are also advantageous in that they protect the metal against corrosion. And they are environmentally friendly and might be favourably used to replace the toxic chromium (VI)-based pigments.

Author details

Kateřina Nechvílová, Andrea Kalendová* and Miroslav Kohl

*Address all correspondence to: andrea.kalendova@upce.cz

Faculty of Chemical Technology, University of Pardubice, Pardubice, Czech Republic

References

[1] A. Kalendova, D. Vesely, M. Kohl and J. Stejskal, Prog. Org. Coat. 78, 1 (2015).

[2] P. Benda and A. Kalendova, Phys. Proced. 44, 185 (2013).

[3] R. Naredi, M. Mahdavian and A. Darvish, Prog. Org. Coat. 76, 302 (2016).

[4] A. Darvish, R. Naredi and M. M. Attar, Prog. Org. Coat. 77, 1768 (2014).

[5] E. Langer, H. Kuczyńska, E. K. Tarnawska and J. Lukastcyk, Prog. Org. Coat. 71, 162 (2011).

[6] M. A. Deyab, Prog. Org. Coat. 85 146 (2015).

[7] X.-Z. Gao, H.-J. Liu and F. Cheng, Chem. Eng. J. 283, 682 (2016).

[8] M. Conradi, A. Koujan, M. Zorko and I. Jerman. Prog. Org. Coat. 74, 392 (2012).

[9] M. E. H. Sadek, R. M. Khattab, A. A. Gaber and M. F. Zawrah, Spectrochim. Acta Part A . 125, 353 (2014).

[10] A. Kalendová, Pigm. Resin Technol. 27, 225 (1998).

[11] A. Kalendová, Anti-Corros. Methods Mater. 45, 344 (1998).

[12] A. Kalendová, Pigm. Resin Technol. 29, 215 (2000).

[13] A. Kalendová, Pigm. Resin Technol. 29, 164 (2000).

[14] L. Anez, S. Calas-Etienne, J. Primera and T. Woignier, Microporous and Mesoporous Mater. 200, 79 (2014).

[15] T. Marzi, Constr. Build. Mater. 97, 119 (2015).

[16] J. Šadauskiene, V. Stankevičius, R. Bliudžuus and A. Gailius, Constr. Build. Mater. 23, 2788 (2009).

[17] M. Ulbrich and A. Kalendova, Phys. Proced. 44, 247 (2013).

[18] J. Du, S. Liang, X. Wang and Z. Fan. Acta Metall. Sinica (English lett.). 22, 263 (2009).

[19] S. Y. Arman, B. Ramezanzadeh, S. Farghadani, M. Mehdijour and A. Rajabi, Corros. Sci. 77, 118 (2013).

[20] B. Nikravesh, B. Ramezanzedeh, A. A. Sarabi and S. M. Kasiriha, Corros. Sci. 53, 1592 (2011).

[21] J.-M. Hu, J.-T. Zhang, J.-Q. Zhang and C.-N. Cao, Corros. Sci. 47, 2607 (2005).

[22] I. Kos, I. G. Schwarz and K. Suton, Procedia Engineer. 69, 881 (2014).

[23] M. Kohl and A. Kalendova. Prog. Org. Coat. 86, 96 (2015).

[24] S. Singh, N. Kumar, R. Bhargava, M. Sahni, K. Sung and J. H. Jung, J. Alloys and Compd. 587, 437 (2014).

[25] L. Lu, I. Swonkaev, A. Kumar and D. V. Goia, Powder Technol. 261, 87 (2014).

[26] S. Roy, S. Kar, B. Bagchi and S. Das, Appl. Clay Sci.107, 205 (2015).

[27] C. Liu, M. Ye, A. Han and J. Li, Ceram. Int. 41, 5537 (2015).

[28] D. Vesely, A. Kalendova and P. Nemec, Sur. Coat. Technol. 204, 2032 (2010).

[29] G. Toussaint, M. Brisbois, J. Grandjean, R. Cloots and C. Menrist, J. Colloid and Interface Sci. 329, 120 (2009).

[30] M. Ren, H. Yin, Y. Hang, C. Ge, Y. Zhang, A. Wang, L. Yu and Z. Wu, Powder Technol. 214, 31 (2011).

[31] J. Li, L. Ecco, M. Fedel, V. Ermini, G. Delmas and J. Pan, Prog. Org. Coat. 87, 179 (2015).

[32] A. Gergely, I. Bertoti, T. Totok, E. Pfeifer and E. Kalman, Prog. Org. Coat. 76, 17 (2013).

[33] A. Kalendová and D. Veselý, Pigm. Resin Technol. 36, 195 (2007).

[34] A. Kalendová and D. Veselý, Anti-Corros. Methods Mater. 54, 3 (2007).

[35] P. Porta, F. S. Stone and R. G. Turner, J. Solid State Chem. 11, 135 (1974).

[36] K. Sun, G. Wu, B. Wang, Q. Zhong, Y. Yang, Z. Yu, C. Wei, X. Jiang and Z. Lan, J. Alloys Compd. 650, 363 (2015).

[37] A. Kalendová, P. Rysanek and K. Nechvilova, Prog. Org. Coat. 86, 147 (2015).

[38] A. L. Fernandez and L. de Pablo, Pigm. Resin Technol. 31, 350 (2002).

[39] M. F. Zawrah, H. Mamaad and S. Meky, Ceram. Int. 33, 969 (2007).

[40] J. B. R. Neto and R. Moreno, Appl. Clay Sci. 37, 157 (2007).

[41] Z. Li, T. Katsumi, T. Inui and A. Takai, Soils Found. 53, 680 (2013).

[42] D. Veselý, A. Kalendova and M. V. Manso, Prog. Org. Coat. 74, 82 (2012).

[43] K. J. Jotti and K. Palanivelu, Appl. Surf. Sci. 288, 60 (2014).

[44] A. Kalendová and D. Veselý, Prog. Org. Coat. 64, 5 (2009).

[45] A. Kalendová, D. Veselý and P. Kalenda, Applied Clay Science 48, 581 (2010).

[46] A. Kalendová, P. Kalenda and D. Veselý, Prog. Org. Coat. 57, 1 (2006).

[47] A. Kalendova, Prog. Org. Coat. 44, 201 (2002).

[48] Y. Hao, F. Liu and E. Man, J. Electrochem. Soc. 159, 403 (2012).

[49] M. Kohl, A. Kalendová, R. Boidin and P. Němec, Prog. Org. Coat. 77, 1369 (2014).

[50] A. Kalendová, D. Veselý, M. Kohl and J. Stejskal, Prog. Org. Coat. 77, 1465 (2014).

[51] A. M. Atta, R. A. El-Ghazawy and A. M. El-Saeed, Int. J. Electrochem. Sci. 8, 5136 (2013).

[52] M. Conradi, A. Kocijan, D. Ker-Merl, M. Zorko and I. Verpoest, Appl. Surf. Sci. 292, 432 (2014).

[53] M. F. Montemor, Surf. Coat. Technol. 258, 17 (2014).

[54] A. Kalendová, Prog. Org. Coat. 38, 199 (2000).

[55] G. Wang and J. Yang, Surf. Coat. Technol. 204, 1186 (2010).

[56] D. Sun, M. X. Wang, Z. H. Zhang, H. L. Tao, M. He, B. Song and Q. Li, Solid State Commun. 223, 12 (2015).

[57] N. M. Ahmed, M. G. Mohamed, M. R. Mabrouk and A. A. ElShami, Construction and Building Mater. 98, 399 (2015).

[58] H. S. Emira and F.F. Abdel-Mohsen, Pigm. Resin Technol. 32, 259 (2003).

[59] A. M. Banerjee, M. R. Pai, S. S. Meena, A. K. Tripathi and S. R. Bharadwaj, Int. J. Hydrogen Energy 36, 4768 (2011).

IntechOpen